

A Bow-Tie Bluetooth/Wimax Antenna Design for Wireless Networks Applications

M. ABRI*, H. BADAOU** and Z. BERBER*

*Laboratoire de Télécommunication, Département de Génie Electrique et d'Electronique
Faculté de Technologie, Université Abou-Bekr Belkaïd –Tlemcen-Algeria

**Laboratoire STIC, Département de Génie Electrique et d'Electronique
Faculté de Technologie, Université Abou-Bekr Belkaïd –Tlemcen-Algeria

Article Info

Article history:

Received July 01th, 2012

Accepted July 22th, 2012

Keyword:

printed bowtie antenna
méthde moments
model the transmission line
Bluetooth
Wimax.

ABSTRACT

The work presented in this paper is focused on the design of printed antennas suitable for wireless networks. The antennas are of bow-tie shape operating in the Bluetooth and Wimax frequency bands. Several antenna configurations have been developed during the various tests and the results obtained by the model of the transmission line have been compared with the moment method of the Momentum software. A perfect agreement was observed between the two models and an excellent result was obtained by the simulated antennas. The optimized antennas has to be integrated on laptops

Copyright © 201x Insitute of Advanced Engineeering and Science.
All rights reserved.

Corresponding Author:

First Author,
Laboratoire de Télécommunication, Département de Génie Electrique et d'Electronique
Faculté de Technologie, Université Abou-Bekr Belkaïd –Tlemcen-Algeria
Email: abrim2002@yahoo.fr

1. INTRODUCTION

Recent years have seen the emergence of a wide variety of wireless networks and a new need was created: that of being constantly connected to a network regardless of where one is. What emerges from many types of networks: telephone networks, broadband distribution, local or sweeping through ground and space communications. Thus, the development of wireless networks requires technological advances in electronic components, computer software, coding techniques or antenna. Indeed, the antenna is one of the key points of wireless networks since this element is the last link in the chain through the emission, transmission and reception of the signal. The telecommunications market has grown considerably since the recent progress in the field of antennas. Users tend to favor the use of lightweight devices, low cost and compact. The printed antennas can largely meet these requirements [1-4].

Their flexible structures and sometimes conformable allow easy integration into various telecommunication systems. However the printed antennas have a very low bandwidth and are often very sensitive to their environment (temperature fluctuations, nearby metal objects ...). These disturbances alter unpredictably the resonant frequency of the antenna, which then becomes much less effective. For this purpose, and because of the applications related to new technologies, the antennas must have a high bandwidth to provide broadband.

In recent years, the subject to broaden the bandwidth of printed antennas has received considerable attention, some techniques such as coupling opening, the use of multilayer structures, thick dielectric substrates enable a bandwidth of 15 % to 55%.

Antenna design for this type of system must meet a specific set of specifications, the first criterion is the impedance matching over the entire allocated frequency band. Omnidirectional radiation character and varies little over this range is also desirable.

Because of their ease of deployment and their relatively low cost, wireless networks are increasingly used. As with wired networks, we usually class wireless networks in their areas of coverage: personal networks WPAN (Wireless Personal Area Networks), local area networks WLAN (Wireless Local Area Networks), Metropolitan Area Networks WMAN (Wireless Metropolitan Area Networks). Characterization of printed antennas requires the use of software using numerical methods as rigorous integral equations solved by the moments method. The latter we certainly offer better accuracy, but require tedious calculations. The use of the transmission line model gives the best solution. Within this framework we will develop an equivalent model fast, simple and precise to account for all geometric characteristics, electrical and technology-node bowtie antennas and their feeds. A fundamental rule of scientific research is validating the results. To do so, a rigorous method of moments was chosen to demonstrate the validity of this model by comparing the results of return loss, VSWR, the reflected phase and the input impedance locus.

2. THE TRANSMISSION LINE MODEL

A bow-tie antenna fed by a microstrip line is represented in Figure 1. In this case, the antenna is fed at the center by a quarter-wave line [5-6]. The two tapers are of different dimensions and in order to allow operation at different frequencies.

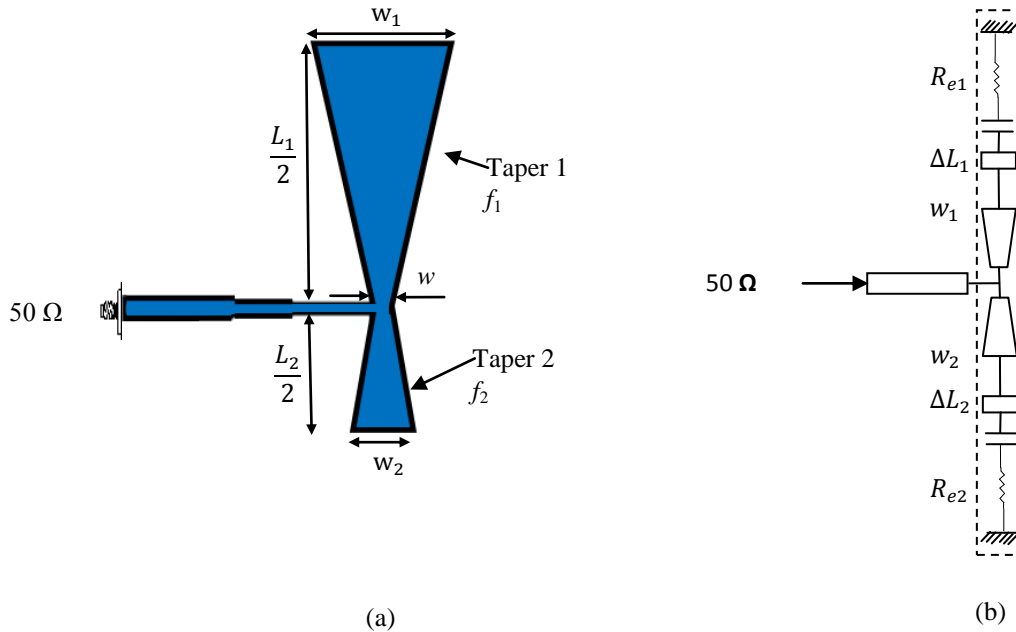


Figure 1. (a) the bowtie antenna mask layout, (b) Equivalent circuit of the multiband antenna.

The extension of normal length is given by the following equation [7-9]:

$$\frac{\Delta L_{1,2}}{h} = 0.412 \frac{(\epsilon_{reff} + 0.3) \left(\frac{W_{1,2}}{h} + 0.264 \right)}{(\epsilon_{reff} - 0.258) \left(\frac{W_{1,2}}{h} + 0.8 \right)} \tag{1}$$

The effective width of the antenna is given by the following formula:

$$W_{1,2} = \frac{1}{2 f_{r_{1,2}} \sqrt{\mu_0 \epsilon_0}} \sqrt{\frac{2}{\epsilon_r + 1}} = \frac{v_0}{2 f_{r_{1,2}}} \sqrt{\frac{2}{\epsilon_r + 1}} \tag{2}$$

The actual length of the antenna can now be determined and is given by the following formula:

$$L_{1,2} = \frac{1}{2 f_{r_{1,2}} \sqrt{\epsilon_{reff}} \sqrt{\mu_0 \epsilon_0}} - 2 \Delta L_{1,2} \quad (3)$$

The input resistance at the edges is given by:

$$R_{e_{1,2}} = \frac{1}{2(G_1 + G_{12})} \left[\cos^2(\beta_g L_{1,2}) + \frac{G_1^2 + B_1^2}{Y_c^2} \sin^2(\beta_g L_{1,2}) - \frac{B}{Y_c} \sin(2\beta_g L_{1,2}) \right]^{-1} \quad (4)$$

2.1. Antenna operating in the Bluetooth frequency band

Figure 2 shows the structure of the antenna designed with a single radiating element of the same size.

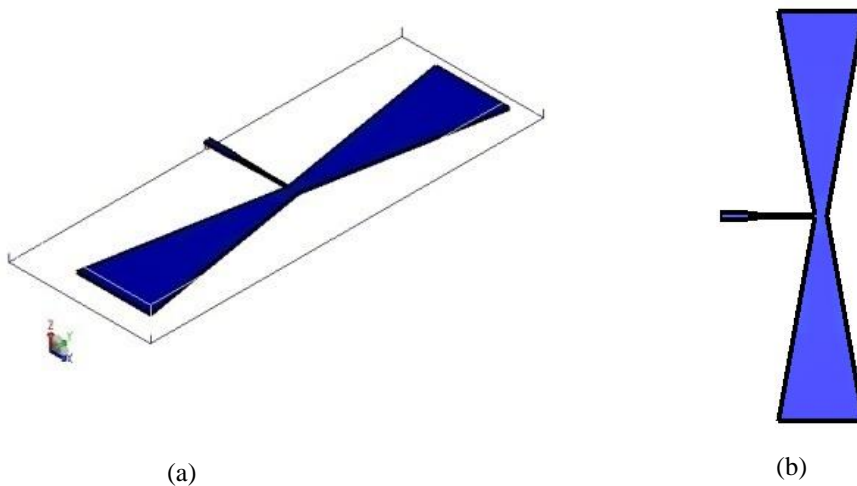


Figure 2. Geometry of the Bluetooth bowtie antenna. (a) Perspective view, (b) Top view.

In this section, we represented the reflection coefficient, input impedance, phase and the standing wave ratio obtained from the simulation of the antenna in the Bluetooth frequency band [2.402 GHz -2.48 GHz].

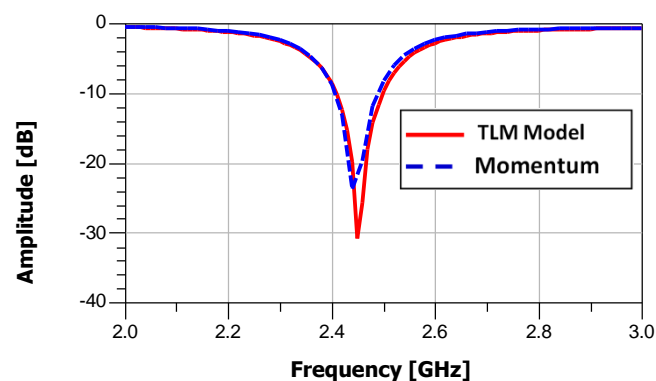


Figure 3. The Bluetooth antenna input return loss.

From Figure 3, there is a very good agreement between both methods (the transmission line model and the method of moments), there was also a perfect network coverage with a desired resonant frequency of 2.44 GHz with a reflection coefficient of about -30 dB.

The Bluetooth antenna input impedance locus on the Smith chart are represented on Figure 4, we see that the results found by the transmission line model is almost identical to that found by the method of moments.

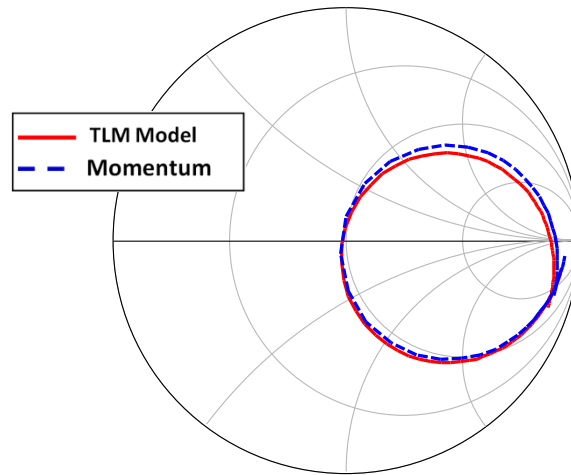


Figure 4. The Bluetooth antenna input impedance locus.

From Figure 4 shown below, there is a perfect superposition of the two curves representing the simulation result of reflected phase at the antenna input by both methods; this phase is zero means that there is a total reflection of the power with absence of standing waves.

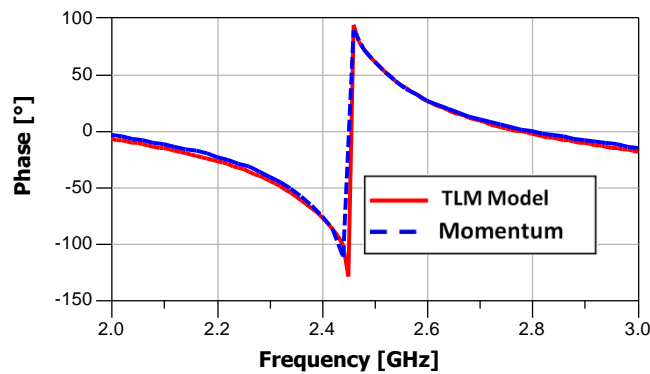


Figure 5. Phase to the input of the Bluetooth antenna.

The standing wave ratio at the input of the antenna by the two methods is shown schematically in Figure 6. Both curves show that the VSWR is equal to 1 at the resonance frequency which means that the antenna matching is perfect.

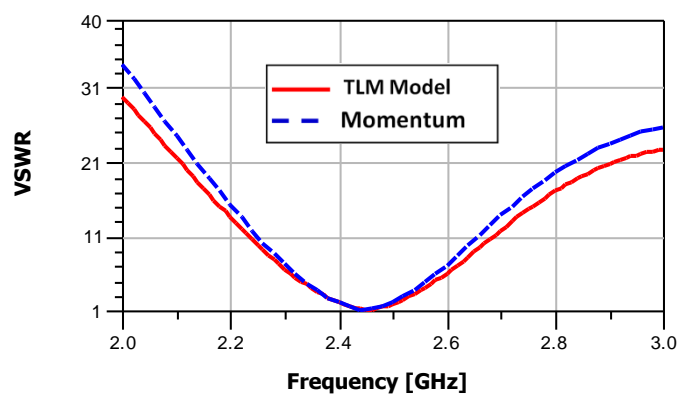


Figure 6. Standing wave ratio at the input of the Bluetooth antenna.

In the figure below, we represent the radiation pattern in 3D at the optimum operating frequency $f = 2.44$ GHz obtained by the method of moments.

From this figure, we see the appearance of two wide lobes due to the geometry of the bowtie antenna.

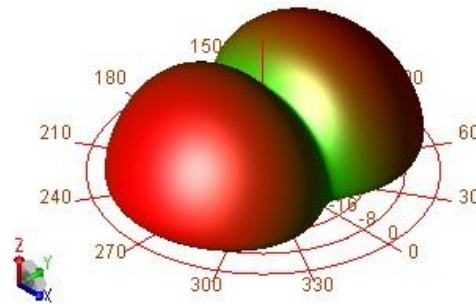


Figure 7. Radiation pattern in 3D of the Bluetooth antenna.

2.2. Antenna operating in the Wimax frequency band

Figure 7 shows the structure of the antenna designed for WiMAX frequency band [3.4-3.6] GHz.

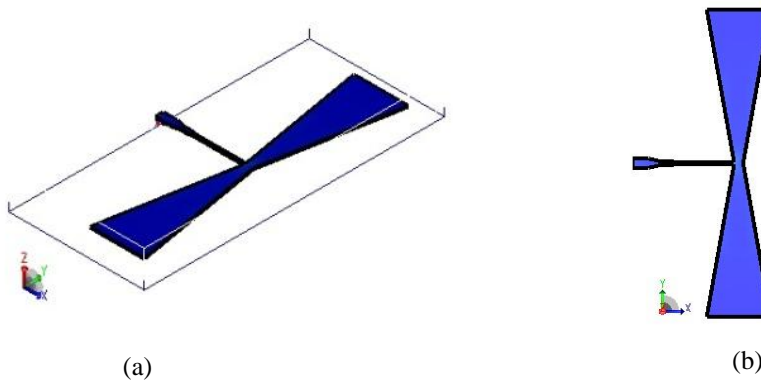


Figure 8. Geometry of the Wimax bowtie antenna. (a) Perspective view, (b) Top view.

The reflection coefficient, input impedance, phase and the VSWR of the antenna are shown below.

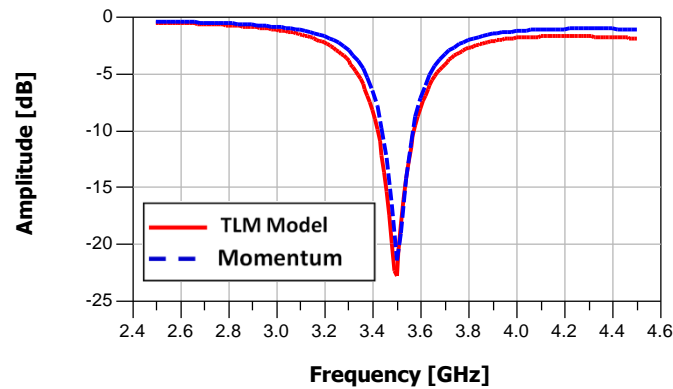


Figure 9. The Wimax antenna input return loss.

The Wimax antenna input return loss is shown schematically in Figure 8, there is a very good network coverage with a peak at 3.5 GHz with S11 equal to -22 dB obtained by the transmission line model and of about - 21 dB in the other model.

Places of input impedance are shown in Figure 9.

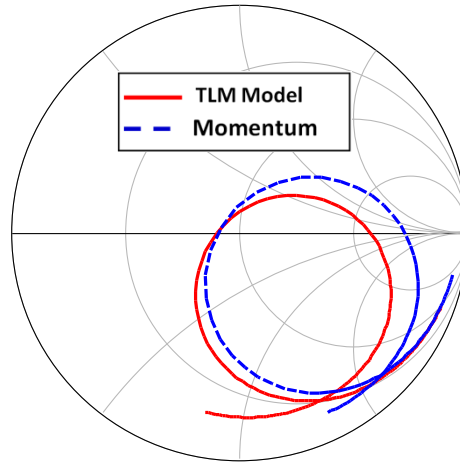


Figure 10. The Wimax antenna input impedance locus.

From the figure above, there is a slight shift by comparing the results found by both models. The simulation result of the reflected phase at the input of the antenna is shown below.

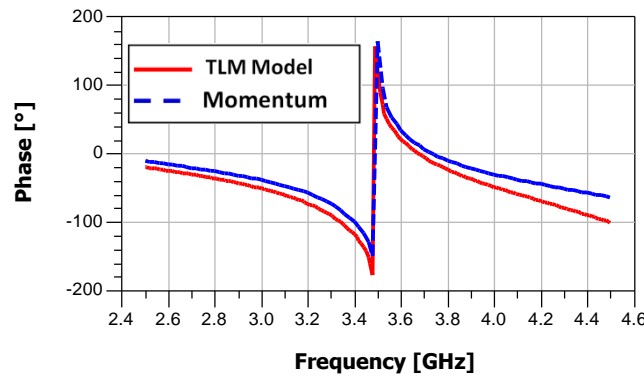


Figure 11. Phase to the input of the antenna Wimax.

In Figure 12, is represented standing wave ratio obtained by both methods of Wimax antenna, it is clear that approaches 1 at the resonance frequency reflecting a perfect matching of the antenna optimized.

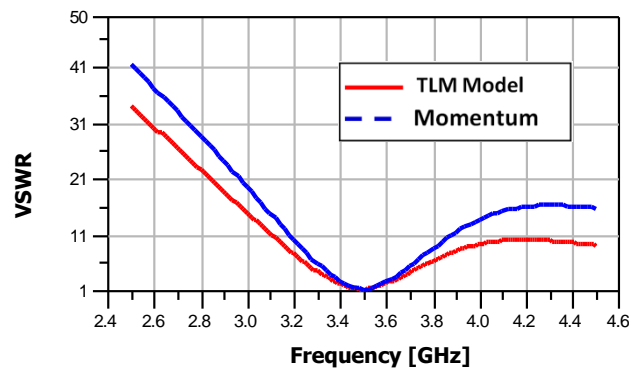


Figure 12. Standing wave ratio at the entrance of the antenna Wimax.

In the figure below, we represent the radiation pattern in 3D at the resonance frequency $f = 3.5$ GHz obtained by the method of moments.

From this figure, we notice the appearance of two lobes large openings due to the geometry of the bowtie antenna.

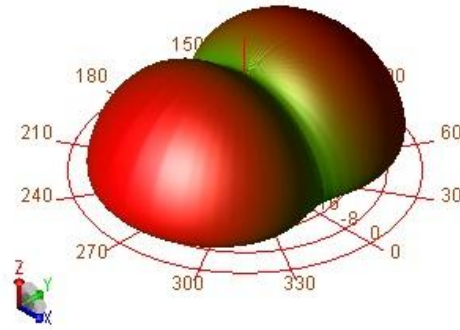


Figure 13. Radiation pattern in 3D of the Wimax antenna.

2.3. Antenna operating in two frequency Bluetooth/Wimax bands.

In this section, we chose to optimize our antenna in two frequency bands, Bluetooth and Wimax. in Figure 14 the structure produced is illustrated:

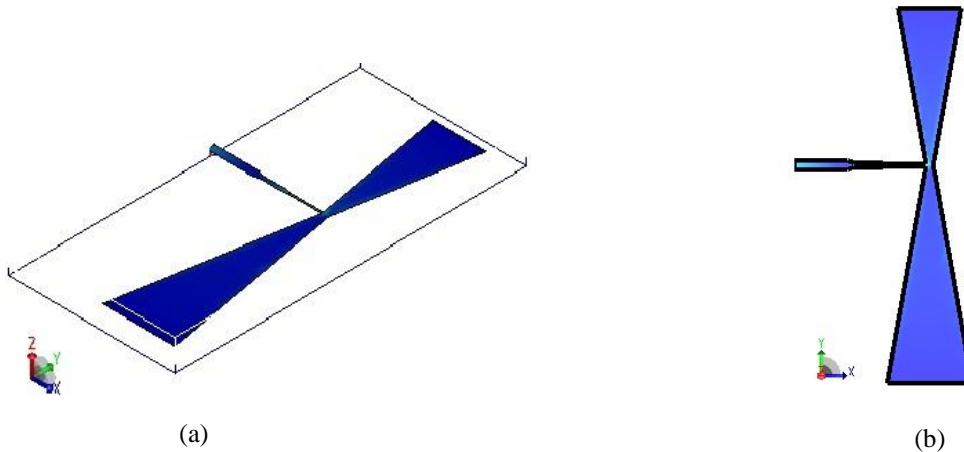


Figure 14. Geometry of the Bluetooth / Wimax. bowtie antenna. (a) Perspective view, (b) Top view.

Here are the results of the input reflection coefficient S_{11} , the reflected phase, the input impedance and VSWR of the simulated antenna.

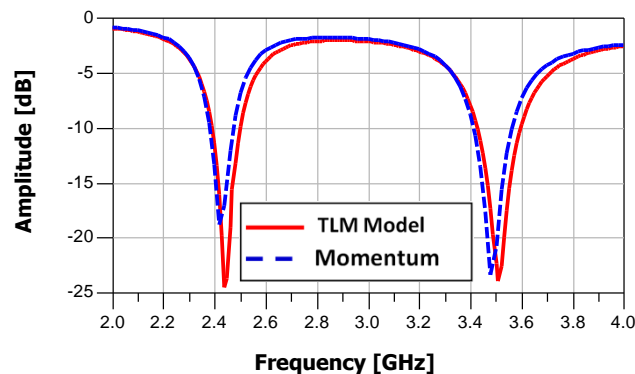


Figure 15. Reflected power to the antenna input Bluetooth / WiMAX

According to the result shown in Figure 15, we see that the resonance of the antenna is correctly predicted at both resonant frequencies, we see two peaks respectively at 2.49 GHz and 3.5 GHz with a reflection coefficient of -25 dB obtained by the transmission line model and a very slight difference obtained at these levels by the moments method.

In Figure 16, it is clear that the results obtained by both methods at the site of input impedance are almost superimposed on each other and give the same value of the input impedance.

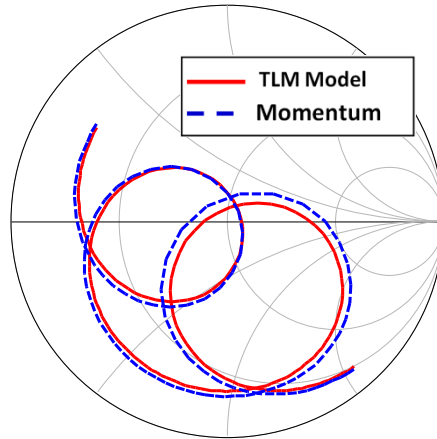


Figure 16. The Bluetooth / Wimax antenna input impedance locus.

Figure 17 illustrates the phase reflected the simulated antenna.

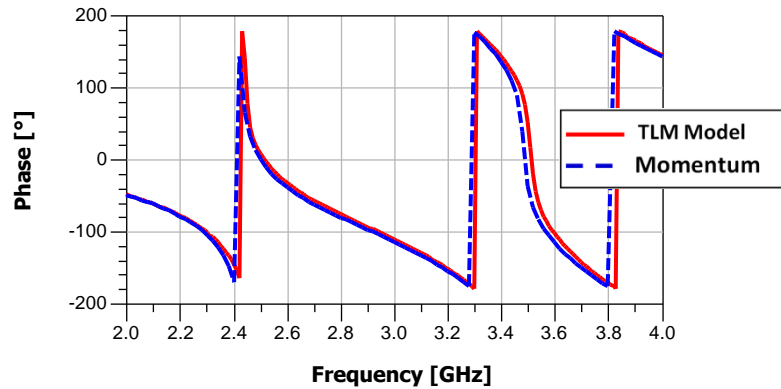


Figure 17. Phase to the input of the antenna Bluetooth / Wimax.

From the figure above, we see reflected a phase zero which results in good adaptation, addition, it is clear that the result found by the method of moments is identical to that of the microstrip line.

The result of the standing wave ratio shown in Figure 18 of this antenna is very good, although there is as resonant frequencies, it tends to 1 which explains why it is ideally suited.

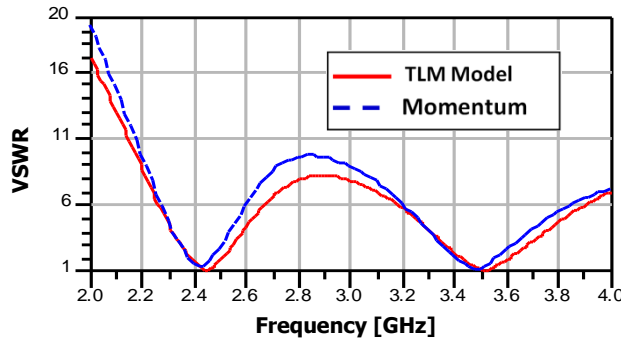


Figure 18. Standing wave ratio of antenna Bluetooth / Wimax.

In Figure 19, we represent the radiation pattern in 3D at the resonance frequencies $f=2.49$ GHz and $f=3.5$ GHz obtained by the method of moments.

From this figure, we notice the appearance of two lobes large openings due to the geometry of the bowtie antenna.

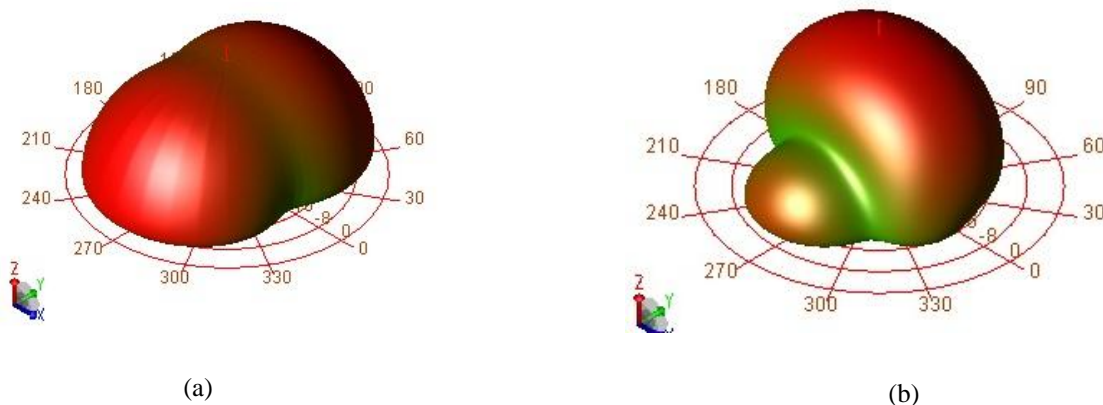


Figure 19. Radiation pattern in 3D. (a) $f=2.49$ GHz, (b) $f=3.5$ GHz.

3. CONCLUSION

The results presented above show the behavior of the antenna for each case studied; we treated the reflection coefficient, input impedance, the reflected phase and standing wave ratio for all frequency ranges covered by the networks Bluetooth, Wimax.

The results obtained by the model of the transmission line were in perfect agreement with those obtained by the moment's method. The model of the transmission line proves its effectiveness in the optimization of the various antennas.

The dimensions and the performance of Bluetooth and WiMax antennas in terms of adaptation and their radiation would be served to be implemented on laptops.

REFERENCES

- [1] M. Abri, N. Boukli-hacene, F. T. Bendimerad, E. Cambiaggio "Design of a Dual Band Ring Printed Antennas Array" Microwave journal., Vol. 49, N°. 5, pp. 228-232, 2006.
- [2] J. F. Zurcher & F. E. Gardiol, Broadband Patch Antenna, Artech House, Boston. London.
- [3] L. Freytag, ' Conception, Réalisation et Caractérisation d'Antennes Pour Stations de Base des Réseaux de Télécommunication Sans Fil ', Thèse de doctorat université de Limoges, Novembre 2004.
- [4] Abri. M., Bendimerad. F. T., Boukli-hacene. N and Bousahla. M., 'Log Periodic Series-Fed Antennas Array Design Using a Simple Transmission Line Model'., International Journal of Communication Engineering Volume 2, Number 3, pp. 161-169, 2009.
- [5] M. Abri, H. Abri Badaoui, S. Didouh and S. M. Bahloul, 'Seven Bow-Tie Antennas Array Design For C Band Applications', congrès mediterraneen des telecommunications et exposition, 22, 23 & 24 Mars 2012, Fes, Maroc.
- [6] S. Didouh, M. Abri and F. T. Bendimerad, 'Multilayered Bow-tie Antennas Design for RFID and Radar Applications Using a Simple Equivalent Transmission Line Model', International Journal of Computer Networks & Communications (IJCNC), Vo. 4, No.3, pp. 121-131, May-June 2012.
- [7] C. A. Balanis, Antenna Theory Analysis and Design, Second Edition, John Wiley and Sons, 1997.
- [8] D. M. Pozar, 'Microstrip Antennas', Proc. IEEE, vol. 80, 1992, pp 79 -91.
- [9] M. Abri, H. Dib and A. S. E. Gharnaout, 'Accurate Model for Single Bow-Tie Antenna Design', International Journal of Microwave and Optical Technology, Vol. 6, N° 5, september, 2011.